Published in IET Microwaves, Antennas & Propagation
Received on 23rd January 2008
Revised on 3rd September 2008
doi: 10.1049/iet-map.2008.0189

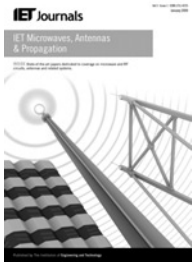

ISSN 1751-8725

Sectorised antenna array and measurement methodology for indoor ultra-wideband applications

Nasimuddin Z.N. Chen X. Qing T.S.P. See
RF and Optical Department, Institute for Infocomm Research, 1 Fusionopolis Way, #21-01, Connexis, Singapore 138632, Singapore
E-mail: nasimuddin@i2r.a-star.edu.sg

Abstract: A new sectorised antenna array (SAA) and measurement methodology are proposed for indoor ultra-wideband (UWB) applications. The proposed SAA comprises of one centre element and six side elements. The one centre element and six side elements are arranged in a semi-spherical antenna array configuration. The measurement system and methodology for the coverage of the SAA are developed. The measured bandwidth of the SAA for voltage standing wave ratio (VSWR) ≤ 2 is 37.5%, ranging from 3.06 to 4.47 GHz. The boresight gain is more than 5.2 dBi across the impedance bandwidth. The proposed SAA is able to provide omni-directional pattern with an average gain of 5.2 dBi over the angles ($0-360^\circ$). The discone reference antenna is used to measure the coverage of the proposed SAA. The proposed measurement study shows that the proposed SAA offers omni-directional coverage desirable in UWB indoor location and short-range communication systems.

1 Introduction

The use of sectorised antennas is common in many wireless applications because they can provide both link and system advantages. Ideal omni-directional antennas transmit and receive equal power in all directions on the horizontal plane as shown in Fig. 1*a*. The drawback of deploying the omni-directional antenna on the ceiling is the poor reception in regions beneath the antenna. Therefore their usage in indoor communications is limited. A possible solution to alleviate this problem is to use an antenna array, which consists of several directional antenna elements. Some improved features such as high scalability and high resource efficiency can be obtained by employing sector antennas in wireless systems. These systems are wireless local area network (WLAN) and *ad hoc*. The design of the ultra-wideband (UWB) microstrip antennas with directional radiation is challenging because of the difficulty in obtaining flat directional radiation over a wide frequency range. In an UWB systems, the operating bandwidth reaches 43% for the lower UWB band of 3.1–4.8 GHz, 45% for the upper UWB band of 6.2–9.8 GHz and 110% for the entire UWB band of 3.1–10.6 GHz [1]. The directional antennas/arrays are designed to increase the capacity and connectivity of *ad hoc* networks [2, 3]. Recently, a compact six-sector antenna employing three intersecting dual-beam microstrip array with common director has been presented for narrow band WLAN applications [4]. The electronically steerable parasitic array radiator antenna for omni-directional and sectoral pattern forming applications to wireless *ad hoc* networks has been proposed [5]. With the use of the sectorised antenna array (SAA) system, the overall system performance can be improved in terms of capacity and spectrum efficiency, therefore achieving the high-data rate in wireless services [6]. UWB techniques have experienced a blooming growth in the past couple of years. Unlike the conventional narrowband communication systems, the UWB occupies a bandwidth of several GHz. Consequently, the antenna implemented in the UWB systems plays an important role than it does in any other system, since it actually acts as a band-pass filter to reshape the spectra of the pulses and hence should be designed carefully to avoid unnecessary distortions. The transmission of power in particular directions by the directional antennas results in a higher degree of spatial reuse of the shared medium. Furthermore, directional transmission utilises

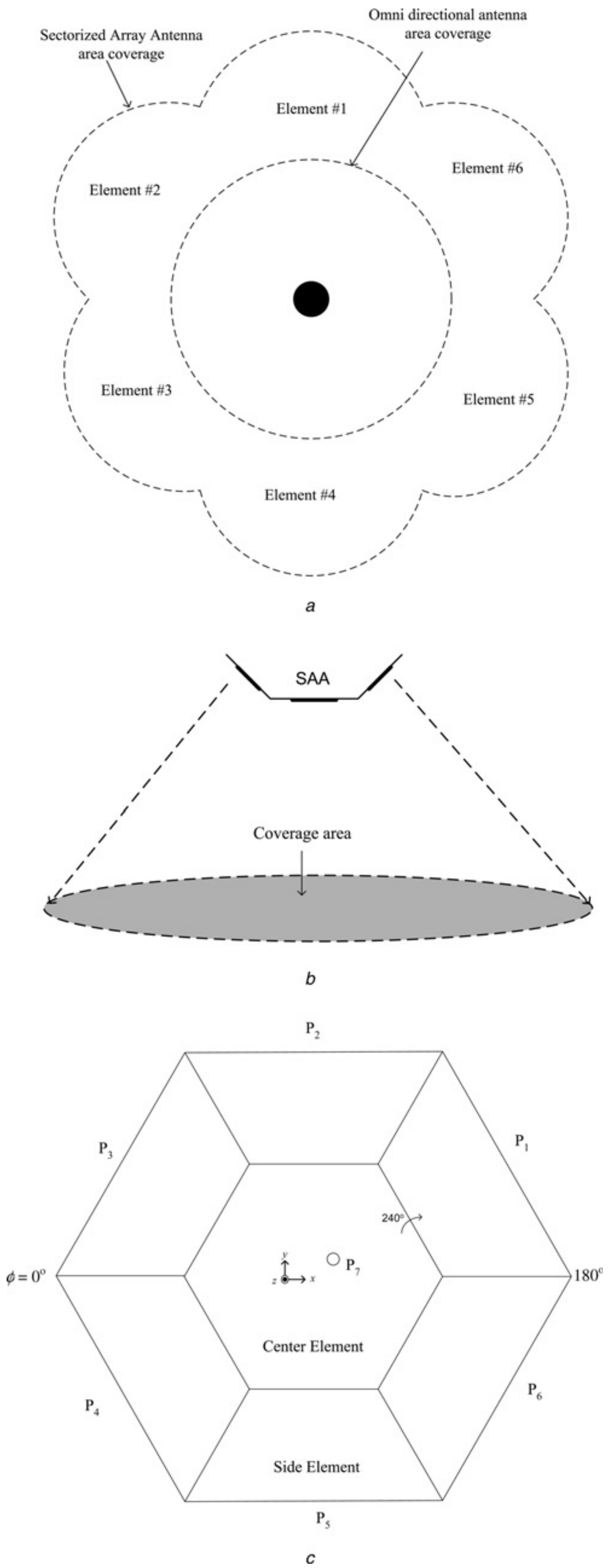

Figure 1 *Coverage of the antennas and proposed SAA configuration*

a Coverage of the omni-directional antenna and the SAA
b Illustration of the desired coverage area of the proposed SAA
c Configuration of the proposed SAA

energy more efficiently and the transmission range of the directional antennas is usually larger than that of the omni-directional antennas. However, there is little literature about SAA system for UWB applications. With the best of our knowledge none used directional SAA system for UWB applications in the open literature. The SAA is configured such that each element directs the available signal power to a specific region, thereby increasing the signal strength within that sector. The elements are arranged in a predefined pattern: polyhedral, cubical, pyramidal, cylindrical or spherical. Each element transmits in a direction that is defined by the physical construction of the SAA. The number of antenna elements required will depend on the half-power beamwidth of each directional antenna element. For example, if the beamwidth of the antenna element is around 60°, six antenna elements are required to cover all directions as shown in Fig. 1*a*. An accurate knowledge of the reception capability of each antenna element is important in the planning process during deployment.

In this paper, we propose a wideband directional SAA, which consists of the seven wideband antenna elements. The measurement methodology develops accurate knowledge of the signal strength of the proposed SAA in specific coverage area with reference discone antenna. The design details of the directional multilayered microstrip antenna elements and SAA are provided. The simulated and measured results are presented as well. The measurement setup and methodology to assess the performance of the SAA in a practical indoor environment are presented. Using the proposed methodology, the measured coverage of the SAA using a reference discone antenna is discussed over the desired coverage area.

2 SAA configuration

Our aim, in this paper, is to design the SAA to provide full coverage of a desired circular area under the antenna for specific indoor applications. The proposed specific coverage area illustration is shown in Fig. 1*b*. The sketch of the proposed SAA is shown in Fig. 1*c*. The side element consists of taper ground plane and the centre element consists of hexagonal ground plane. The six side elements are formed as a hollow semi-spherical configuration as shown in Fig. 1*c*. Fig. 1*c* also shows the coordinate system of SAA. The proposed SAA can be put on the ceiling of the indoor. The *z*-direction of the SAA is just right below the ceiling. The two side elements with the pairs are oriented at 60° to each other such that each separate antenna element covers a sector around 60°, so that the SAA with six side elements creates full 360° coverage horizontally. Since the six side antenna elements are equally distributed around 360°, each side element needs to provide 60° beamwidth with directional radiation. Each side element is provided a coverage area around 60° beam as shown in Fig. 1*a*. The centre element is designed to cover the area just right below the SAA, which is helpful to

doi: 10.1049/iet-map.2008.0189

enhance the field intensity of the SAA in the desired area. The centre element also needs beamwidth around 60° to cover the area just below the SAA. The centre element is able to cover the area just right below the SAA with around 60° beam. The area coverage right below the centre element depends on beamwidth and height of the SAA from the reference antenna. The dimensions of the ground planes for the elements are given in Table 1. All dimensions provided in Table 1 are in millimetre.

3 Antenna elements design

3.1 Antenna elements configuration

The cross-sectional view of the side antenna element and centre antenna element is shown in Fig. 2*a*. The antenna element comprises of a driven patch and four stacked parasitic patches. The feeding structure consists of microstrip line with via for side element. The driven patch with microstrip line-via feed couples the electromagnetic energy to the stacked parasitic patches. The side antenna element consists of three dielectric substrate layers. The microstrip line is printed on Layer #1, the driven patch is printed on Layer #2 and the four parasitic patches are printed on dielectric substrate Layer #3. The centre element is fed by direct coaxial feed to driven patch and four parasitic patches are electromagnetically coupled with driven patch. The ground plane size of the antenna elements is selected based on the proposed SAA as shown in Fig. 1*c*. The ground plane and top view of both the elements are shown in Fig. 2*b*. The chamfered edge length of all the patches, q_d, is shown in Fig. 2*b*. A copper wire via of radius r connects the microstrip feed line and the driven patch for side element. The distance between the centre of via and centre of the driven patch is X_o. The distance from open end of the microstrip line to centre of the driven patch, s, can be varied for impedance matching. The distance between the centres of the parasitic patches is d. The coaxial feed location on ground plane and driven patch is X_o from the centre of the driven patch for the centre element. The specified impedance bandwidth and gain performance can be achieved by optimising the position of the parasitic patches relative to the driven patch [7]. The antenna elements are designed and optimised with the help of the design rules described in [7]. Both antenna elements are optimised for wide impedance bandwidth and desired beamwidth with directional radiation at boresight. The elements designed and optimised dimensions are given in Table 1.

3.2 Results

The measured and simulated VSWR and gain of the side element are shown in Fig. 3. The measured impedance bandwidth (VSWR $\leq$ 2) is 39.3% (3.05–4.54 GHz) and simulated bandwidth is 42% (3.03–4.64 GHz). Good agreement between the simulated and measured results is achieved. The boresight gain is more than 5.2 dBi across the impedance bandwidth. Fig. 4 shows the VSWR and boresight gain with frequency of the centre element. The measured impedance bandwidth (VSWR $\leq$ 2) is 37.5% (3.06–4.47 GHz) and simulated bandwidth is 39.6% (3.0–4.48 GHz). The direct coaxial-fed centre element has slightly less impedance bandwidth compared to the side element feed by microstrip-via combination. Both the designed elements are fabricated and tested. The measured boresight gain is greater than 6.0 dBi across the impedance bandwidth, which is slightly higher than that of the side element because of the larger ground plane. Good agreement between the measured and the simulated results is achieved. The impedance bandwidth of the centre element is lower than side element because of used different feeding structures.

Table 1 Designed parameters and dimensions of the antenna elements

Parameters	Side element	Centre element
ε_{r1}, ε_{r2}, ε_{r3} tan δ_1, tan δ_2, tan δ_3	3.38, 3.38, 3.38 0.0027, 0.002, 0.0027	3.38, 3.38, — 0.0027, 0.0027, —
h_1, h_2, h_3	0.81, 2.34, 3.05	3.15, 3.05, —
L_1, L_2	21.5, 17.0	21.5, 17.0
W, W_1, W_2	1.6, 0.9L_1, 0.9L_2	—, 0.9L_1, 0.9L_2
r	0.5	—
X_o	6.05	6.5
s	0.25	—
q_d	3	3
d	30.1	30.1
total height	6.20	6.20
ground plane size	$G_1 = 120.0$, $G_2 = 67.08$, $G_3 = 60.0$	$G_3 = 60.0$

doi: 10.1049/iet-map.2008.0189

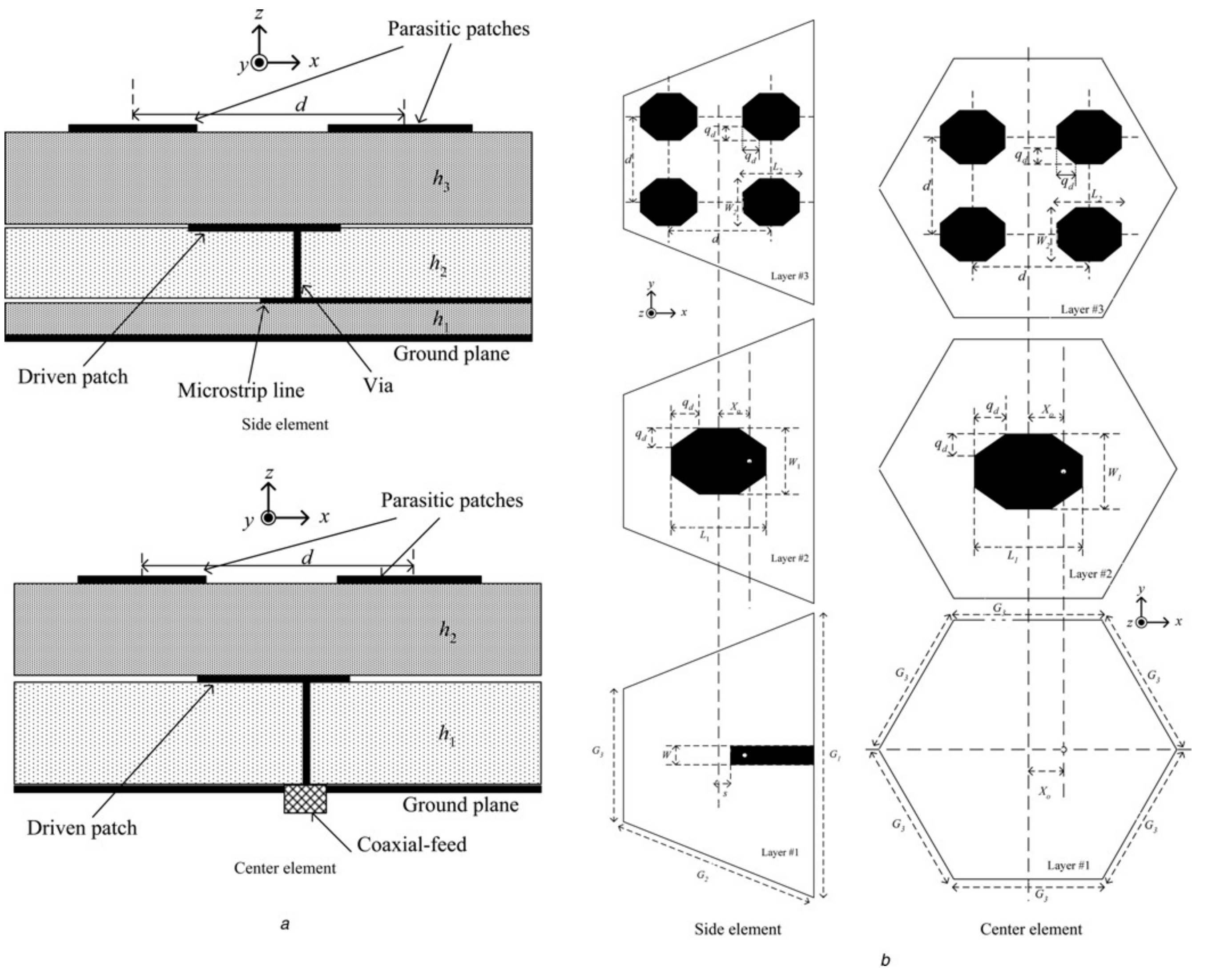

Figure 2 *Geometry of the multilayered microstrip antenna elements (side and centre element)*

a Cross-sectional view
b Top view

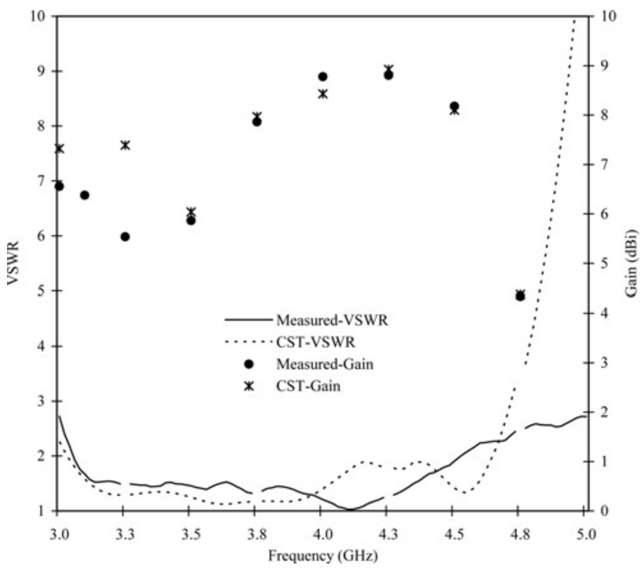

Figure 3 *VSWR and gain of the side antenna element*

The radiation patterns of both the elements are measured from 3.0 to 5.0 GHz at an interval of 0.25 GHz and good agreement with the simulated results is observed. For brevity, only the measured normalised radiation patterns of the antenna at 3.0, 4.0 and 4.5 GHz are shown in Fig. 5*a* for centre element and Fig. 5*b* for side element, respectively. The cross-polarisation of the elements is also included. Both the elements have almost similar radiation patterns in both planes (*yz* and *xz*). The measured half-power beamwidths are, respectively, around 59° for the side element and 55° for the centre element. In the *xz*-plane, the radiation patterns for the side and centre elements experience a squint of around 18 and 12° from the boresight, respectively, as shown in Fig. 5. This is because of the asymmetric current distribution over the patches. Compared to the co-polarisation levels of both the elements, the maximum cross-polarisation level is lower than −20 dB over all the frequencies within the bandwidth and in both planes. The co-polarisation takes place when

doi: 10.1049/iet-map.2008.0189

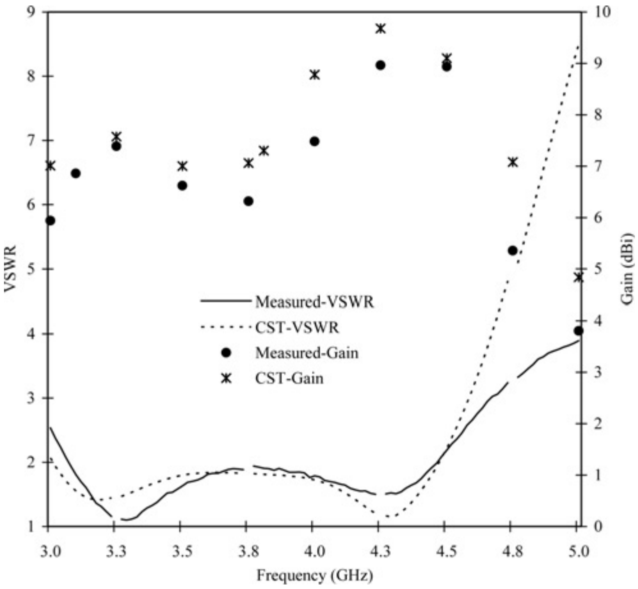

Figure 4 *VSWR and gain of the centre antenna element*

both the reference antenna and the test antenna are in same polarisation. The cross-polarisation takes place when the reference antenna has opposite polarisation compared to the test antenna polarisation. The fabricated proposed SAA is shown in Fig. 6. The return loss and isolation of the fabricated SAA were tested. The mutual coupling between the elements, or $|S_{21}|$, is lower than -23 dB for both cases (side–side elements and side–centre elements). The impedance performance of all the elements remains nearly unchanged within the frequency range of 3.06–4.47 GHz. All the sectors of the SAA can be excited at a time or one sector at a time depending on the applications.

4 Measurement methodology and setup

The transmission signal level or field strength over a specific coverage area of the SAA is an important and useful information for indoor system designing and deployment. Therefore it is necessary to develop an efficient measurement method to obtain the signal levels within a specific coverage

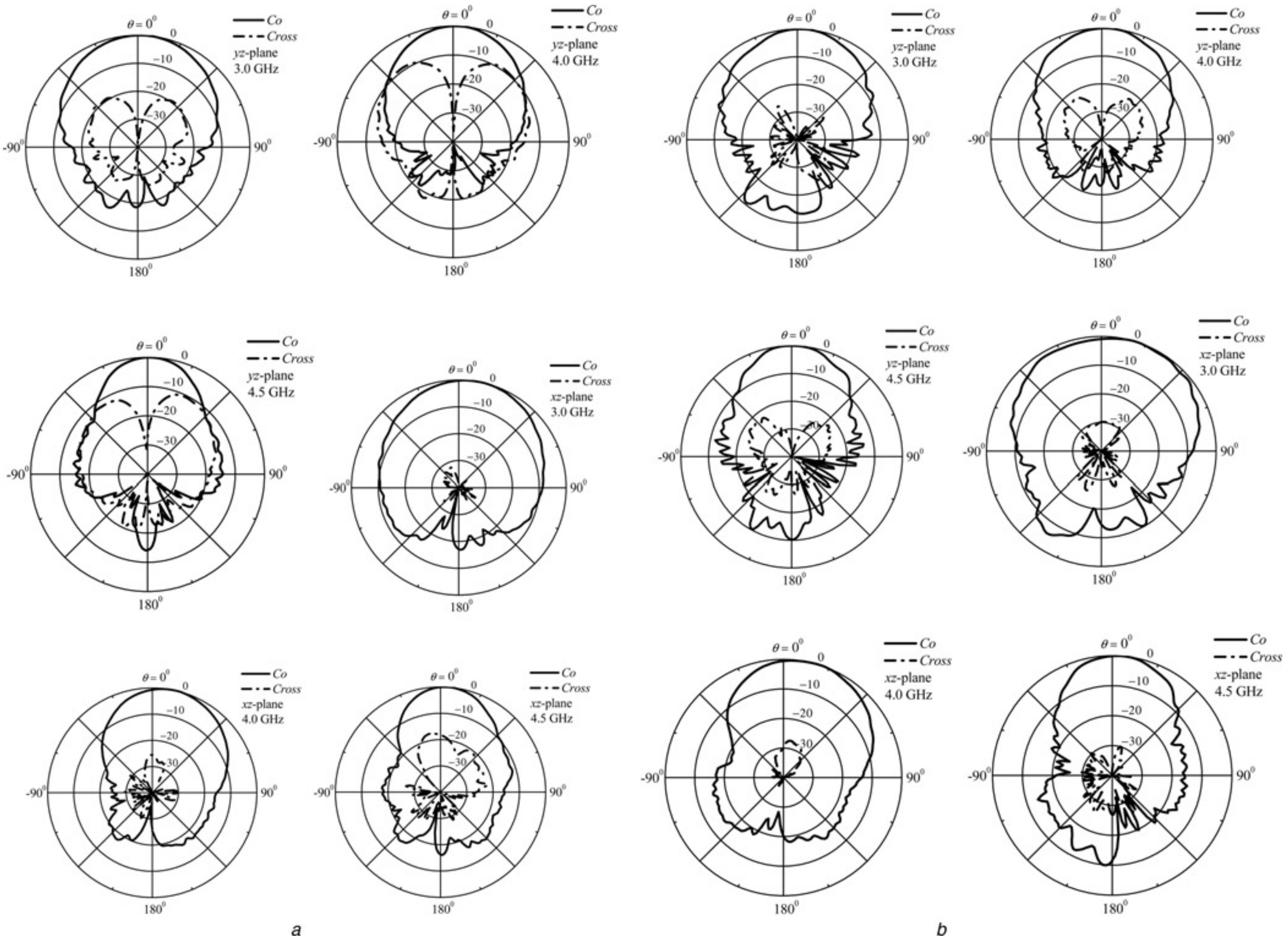

Figure 5 *Measured normalised radiation patterns at 3.0, 4.0 and 4.0 GHz for both planes (xz and yz)*

a Centre element
b Side element

area of the SAA as shown in Fig. 1*b*. The measurement methodology was studied and a measurement setup was developed as shown in Fig. 7*a*. The measurement setup is located in the workshop at the Institute for Infocomm Research, Singapore. This location was selected because of the large amount of potential multipaths from the nearby scatters and is therefore representative of a typical dense indoor environment. The length of the slider is 280 cm, with the centre of the slider marked at $d = 0$ cm. The reference antenna was mounted on an 88 cm high stand from the base of the slider bench. The shortest distance between the SAA and the reference antenna is 130 cm, which occurs when $d = 0$ cm as shown in Fig. 7*b*. The proposed SAA was mounted on a frame which is above a slider, the reference antenna was installed on a slider and moved by a programmed motor. The amplifier was used to improve the signal level. The SAA and reference antenna were connected via cables to ports of a vector network analyzer (VNA), the signal or field strength is indicated by the amplitude of measured S_{21}. The metallic parts of the frame were covered with absorber to reduce the reflections from the metallic frame parts. By rotating the SAA from $\phi = 0$ to 180° in the horizontal plane and moving the reference antenna along the slider, the signal levels within the circular coverage area under the antenna can be obtained. So proposed measurement methodology is able to measure the full coverage under the antenna.

In the measurements, the SAA is rotated in steps of $\phi = 20^\circ$ in the horizontal plane and the slider is moved in steps of 20cm from $d = -140$ to 140 cm. The movement of the reference antenna on slider is electronically controlled by the computer. In Fig. 7*c*, each spots on the circle with respect to the centre of the slider represent the location of the reference antenna within the coverage area. For instance, with the SAA at $\phi = 0^\circ$, by moving the reference antenna from $d = -140$ to 140 cm, the $|S_{21}|$ can

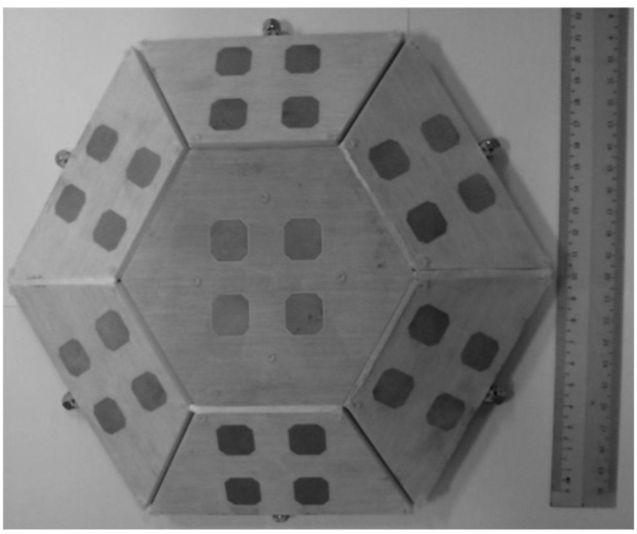

Figure 6 *Fabricated proposed SAA prototype*

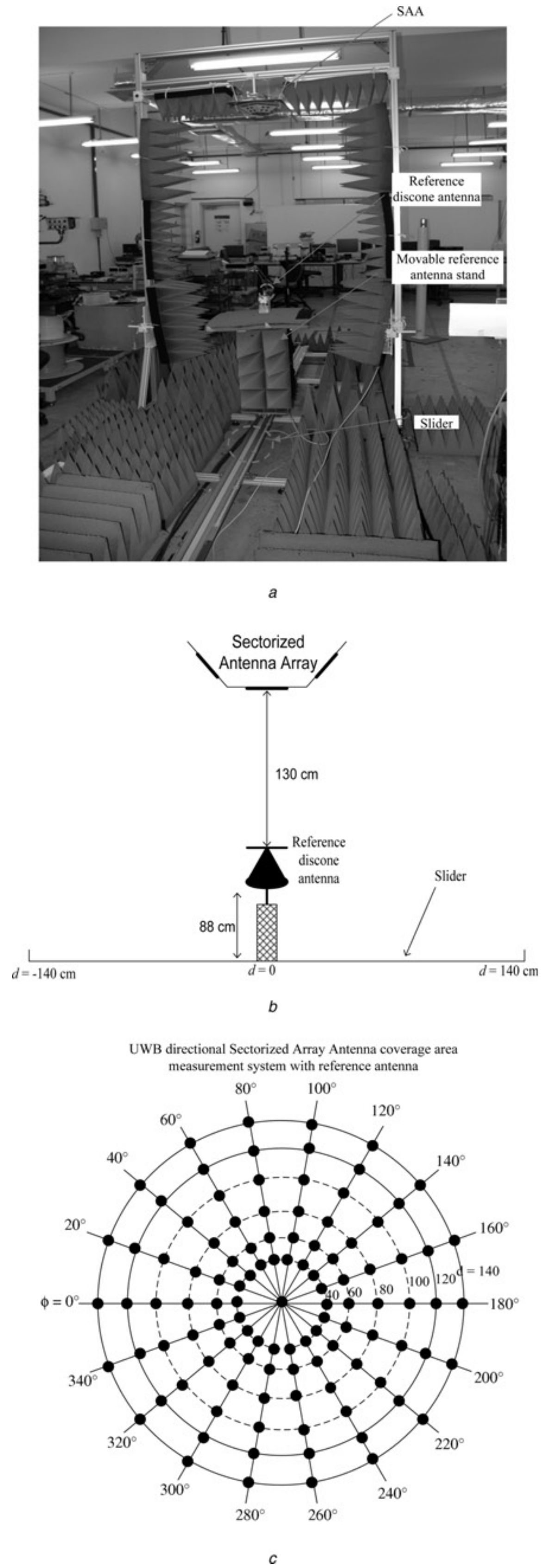

Figure 7 *Measurement setup of the coverage for a SAA*

a Photo of the measurement setup in workshop
b Diagram of measurement setup of the SAA and reference antenna
c Measurement points within the coverage area of the SAA

IET Microw. Antennas Propag., 2009, Vol. 3, Iss. 4, pp. 621–629
doi: 10.1049/iet-map.2008.0189

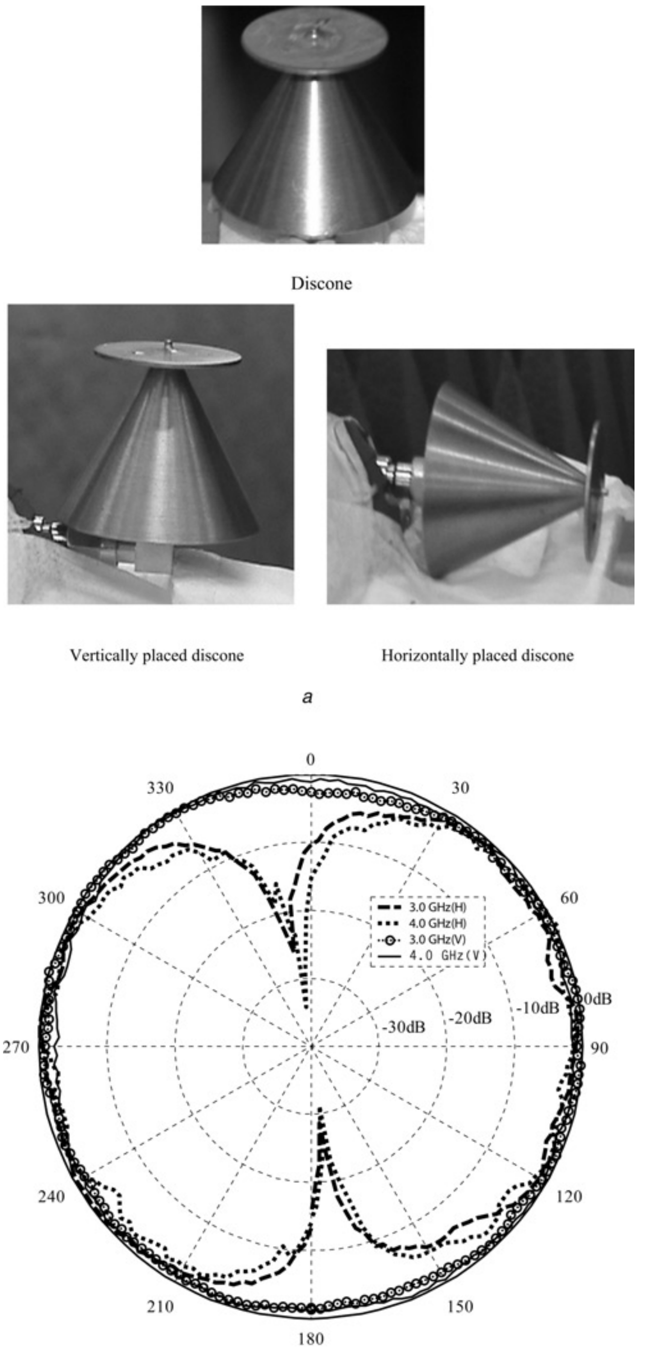

Figure 8 *Reference discone antenna*

a Discone and vertically/horizontally placed discone
b Measured radiation patterns in vertical and horizontal planes of the reference discone antenna

be measured along the straight path from $\phi = 0$ to 180° and so on.

5 Measurement results and discussions

The transmission measurement of the SAA was performed using the Agilent VNA N5230A within a frequency range

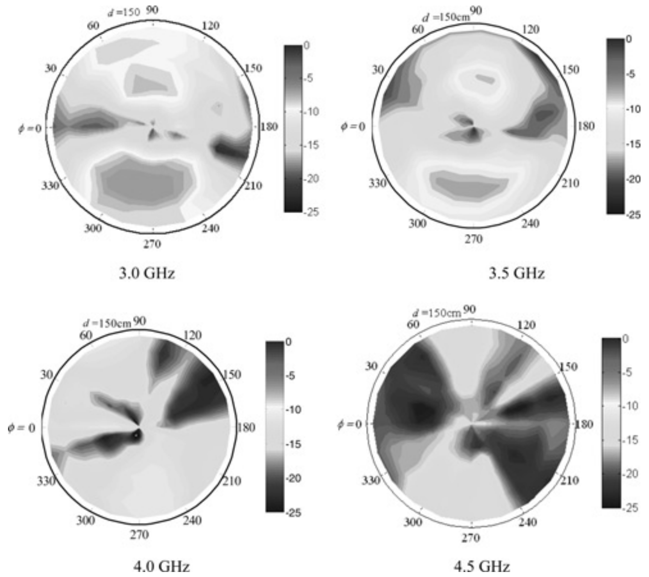

Figure 9 *Measured $|S_{21}|$ between the centre element of SAA and vertically placed discone*

of 3.0–5.0 GHz in a step of 10 MHz using the discone reference antenna. The discone antenna shown in Fig. 8*a* has desirable impedance matching and gain over the UWB band of 3.0 − 10.6 GHz [8]. The discone antenna placed in the vertical and horizontal orientations with respect to the ground plane are also shown in Fig. 8*a*. The measured radiation patterns in vertical and horizontal planes of discone are shown in Fig. 8*b*.

5.1 Centre element

The centre element (P_7) of the SAA was excited and other six elements of the SAA were terminated with 50 Ω terminators. The signal level within a circular area of a 140 mm radius

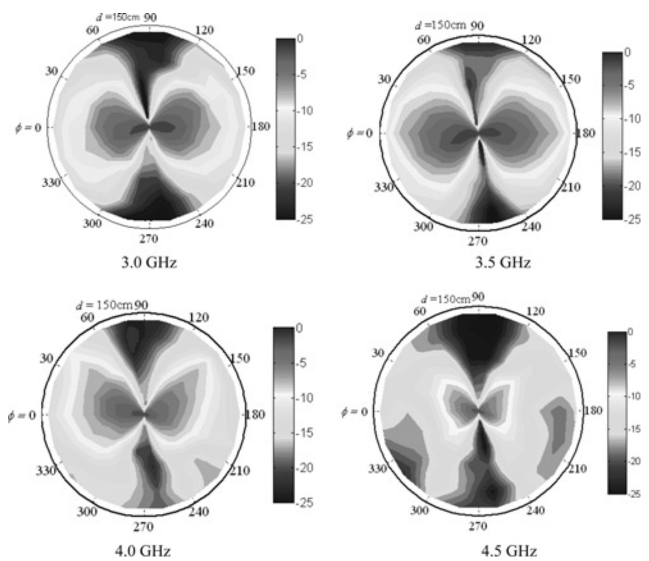

Figure 10 *Measured $|S_{21}|$ between the centre element of SAA and horizontally placed discone*

when the discone is vertically and horizontally placed was measured. The signal level within the coverage area was normalised with the highest signal level ($|S_{21}|$) achieved over the coverage area, that is -17.6 dB. The colourbar with all figures shows scale of the coverage signal strength ($|S_{21}|$) in dB of the SAA with reference discone antenna.

Fig. 9 shows measured $|S_{21}|$ at 3.0, 3.5, 4.0 and 4.5 GHz of the centre element using vertically placed discone. When the SAA is oriented at $\phi = 0/180^\circ$, it is symmetric with respect to both sides of the desired coverage. Because of the orthogonal polarisations of the discone and the SAA, the signal levels are generally low. As there is a deep radiation null when the discone is beneath the SAA, the poor signal reception appears in the blue regions around the centre of the coverage area. Therefore the centre element is able to provide about 60° coverage over the specific area. Since the discone has a deep radiation null when it is placed at the bottom of the SAA, therefore in order to evaluate the coverage capability of the centre element for a SAA, the discone antenna is mounted horizontally on the antenna stand as shown in Fig. 8*a*. The vertical and horizontal radiation patterns of the discone are shown in Fig. 8*b*. The measured $|S_{21}|$ of the SAA is shown in Fig. 10. As the SAA is co-polarised with the discone, the $|S_{21}|$ is very strong along the $\phi = 0/180^\circ$ direction. In this case, the signal strength is high when the discone is directly beneath the SAA. Some yellow and green spots on undesired coverage of the sector element are because of the reflections from the walls of the room.

5.2 Side element

The side element (P_3) of the SAA is excited and the measured $|S_{21}|$ of the SAA with the vertically placed discone is shown in Fig. 11. The signal level within the coverage area was normalised with the highest signal level ($|S_{21}|$) achieved over the coverage area, that is -17.6 dB. The one side element of the SAA is able to cover the sector of 60° well, which is desirable as seen from Fig. 1. Therefore the SAA with the six side elements is able to cover all directions with the vertically placed discone, except for the region right below the SAA. As observed from Fig. 12, when the discone is horizontally placed, the coverage area is shifted along the $120/300^\circ$ direction. This is because of the co-polarised radiation between the side element P_3 of the SAA and the discone. However, the signal strength between the adjacent side elements decreases more rapidly with frequency and range as compared to the centre element when the discone is horizontally placed. Also, as compared to the vertically placed discone, the signal strength below the SAA is stronger when the discone is horizontally oriented but decreases with an increase in frequency.

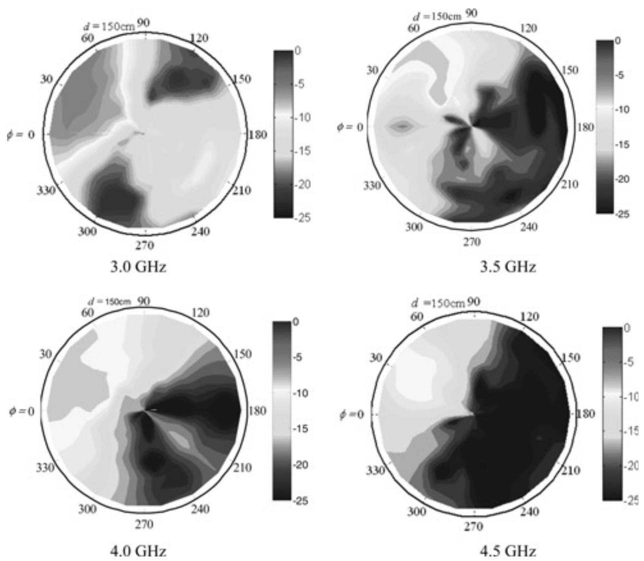

Figure 11 *Measured $|S_{21}|$ between the side element of SAA and vertically placed discone*

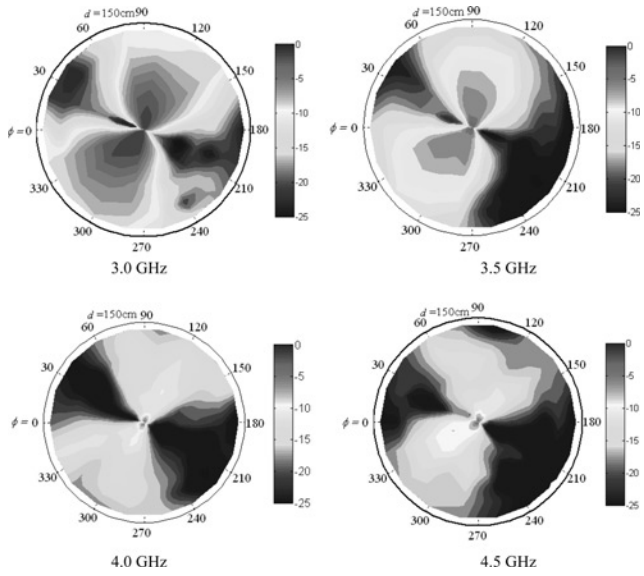

Figure 12 *Measured $|S_{21}|$ between the side element of SAA and horizontally placed discone*

6 Conclusions

This paper has presented the design of a UWB SAA. The measurement methodology of measuring the signal strength in a specific coverage of the SAA in a practical indoor environment has been studied and a measurement setup has been developed. Using the discone UWB reference antenna, the coverage of the proposed SAA has been evaluated. The measured results have shown that the SAA is able to provide coverage over the desired circular coverage across the operating bandwidth when all the elements are excited. The proposed SAA technology allows seven symmetric directional beams to be placed in the single antenna count and simplified antenna alignment at deployment. The investigation has demonstrated that the SAA can be used for

doi: 10.1049/iet-map.2008.0189

UWB high-data rate indoor communications and UWB low-data rate indoor location requesters.

7 Acknowledgments

The authors would like to thank Dr. Wee Kian Toh for his assistance and insight to this research work.

8 References

[1] First Report and Order, Federal Communications Commission (FCC), February 14, 2002

[2] RAMANATHAN R.: 'On the performance of beam forming antennas in ad hoc network', MobiHoc, October 2001

[3] RAMANATHAN R., REDI J., SANTIVANEZ C., WIGGINS D., POLIT S.: 'Ad hoc networking with directional antennas: a complete solution', BBN Technical Report, 2003

[4] HONMA N., SEKI T., NISHIKAWA K., TSUNEKAWA K., SAWAYA K.: 'Compact six-sector antenna employing three intersecting dual-beam microstrip yagi-uda arrays with common director', *IEEE Trans. Antennas Propag.*, 2006, **54**, (11), pp. 3055–3061

[5] CHENG J., HASHIGUCHI M., IIGUSA K., OHIRA T.: 'Electronically steerable parasitic array radiator antenna for onmi- and sector pattern forming applications to wireless ad hoc networks', *IEE Proc. Microw. Antennas Propag.*, 2003, **150**, (4), pp. 203–208

[6] DOUFEXI A., ARMOUR S., NIX A., KARLSSON P., BULL D.: 'Range and throughput enhancement of wireless local area networks using smart sectorized antennas', *IEEE Trans. Wirel. Commun.*, 2004, **3**, (5), pp. 1437–1443

[7] NASIMUDDIN, CHEN Z.N.: 'Wideband microstrip antennas on sandwich substrate', *IET Microw. Antennas Propag.*, 2008, **2**, (6), pp. 538–546

[8] QING X.M., CHEN Z.N., CHIA M.Y.W.: 'UWB characteristics of disc cone antenna'. IEEE Int. Workshop on Antenna Technology: Small Antennas and Novel Materials, Singapore, March 2005, pp. 97–100

doi: 10.1049/iet-map.2008.0189